*Desalination and Water Treatment*
www.deswater.com
doi: 10.1080/19443994.2016.1156029

57 (2016) 25421–25434
November

Taylor & Francis
Taylor & Francis Group

# Modified PID control with $H_\infty$ loop shaping synthesis for RO desalination plants

Bui Duc Hong Phuc[a], Sam-Sang You[b,*], Tae-Woo Lim[c], Hwan-Seong Kim[d]

[a]*Department of Convergence Study on the Ocean Science and Technology, Korea Maritime and Ocean University, Busan 606-791, South Korea, Tel. +82 51 4104971; email: buiduchongphuc@kmou.ac.kr*
[b]*Division of Mechanical Engineering, Korea Maritime and Ocean University, Busan 606-791, South Korea, Tel. +82 51 4104366; email: ssyou@kmou.ac.kr*
[c]*Division of Marine Engineering, Korea Maritime and Ocean University, Busan 606-791, South Korea, Tel. +82 51 4104256; email: kyunlim@kmou.ac.kr*
[d]*Division of Logistics, Korea Maritime and Ocean University, Busan 606-791, South Korea, Tel. +82 51 4104334; email: kimhs@kmou.ac.kr*

Received 18 October 2015; Accepted 13 February 2016

ABSTRACT

This paper deals with the PID control synthesis with robust ($H_\infty$) loop shaping framework to manage MIMO reverse osmosis (RO) desalination plants. This new method takes advantage of the robust controller which has a fixed low order of conventional PID scheme guaranteeing robust stability and performance under large parametric uncertainties, external disturbances, and sensor noises. The coprime factor uncertainty description in $H_\infty$ loop shaping methodology can cover a wide variety of uncertainties over all frequencies for the RO plants. The test results demonstrate that the achieved controller has high stability margin, showing disturbance and noise attenuation abilities. Furthermore, most interactions between control channels have been decoupled in the complete control system. The presented control approach can help reduce membrane cleaning, save energy, and reduce product water costs for the RO plants. Note that weather changes increase unstableness in RO plants but the water treatment facilities are only dimensioned for PID control. In addition, this study addresses control robustness as well as performance of a RO system against uncertainties, disturbances, and noises. Finally, the present control method can be utilized for efficiently controlling water quality (including quantity) and managing water facility of the RO desalination plants.

*Keywords:* $H_\infty$ loop shaping; Proportional-integral-derivative (PID) controller; Multi-input multi-output (MIMO); Quality water; Reverse osmosis (RO); Desalination plants; Robust control

## 1. Introduction

It is known that all of terrestrial life depends on freshwater. Miraculously, just a small percentage of the water on earth is actually available as freshwater. Desalination is a water purification process that removes dissolved minerals (but not limited to salt) from seawater, brackish water, or treated wastewater, leaving behind fresh and potable water. The reverse

*Corresponding author.

osmosis (RO) is the passage of water through a semipermeable membrane from a solution of high salinity to another one with lower salt concentration, overcoming the osmotic pressure due to a driving force. In recent years, the market share of RO water desalination has widely expanded due to significant improvements and advantages in membrane technology [1]. The RO plants offer lower energy consumption, investment cost, space requirements and maintenance than other desalination processes such as multi-stages flash and multi-effect distillation [2].

The performance of RO desalination system is very sensitive to the plant operating conditions and external disturbances. For example, because of fouling, membrane cleaning has to be carried out often and process parameters obtained before and after cleaning are significantly different. Depending water sources, some exhibit greater variations in environmental parameters than other sources. It is known that the membranes are deeply affected by feed water temperature, salinity and other environmental factors [3]. Therefore, the desalination plants often operate under parametric uncertainties and exogenous disturbances. Besides, the global climate change makes desalination plants even more unstable. This means that RO desalination plant requires an efficient and accurate control system to maintain its operation close to the optimum conditions, which result in increased productivity and prolonging the life of the membranes due to the reduction and prevention of membrane fouling and maintenance [4]. Although there are more challenges in controlling RO system, most plant manufacturers currently use conventional control strategy such as classical PID controller. The reason is that the hardware and software available in RO systems were only dimensioned for some simple controllers [5].

In the literature review of RO system, the first PID controller is redesigned into multiple single-input single-output (SISO) structures by Alatiqi et al. [6] for MIMO control strategy. However, the conventional PID controllers generally do not guarantee the robustness and performance against uncertainties and disturbances. Especially it is also very sensitive to measurement noises. Besides, the multiple SISO structure often ignores interactions between different channels in MIMO systems. Based on classical PID, other researchers have developed various control approaches, such as Kim et al. [7] applied Immune-Genetic Algorithm to get PID parameters for RO system, Gambier and Badreddin [5] designed multi objective optimization based PID controller so that the control loop was less sensitive to parameter variations, and Rathore et al. [8,9] and Chithra et al. [10] used Particle Swam Optimization and Luus–Jaakola to tune PID parameters for the controller. Nevertheless, the effects of parametric uncertainties, exogenous disturbances and measurement noises are not sufficiently considered on RO plant control synthesis so far.

Of all control methods to simultaneously deal with uncertainties, disturbances and noises, the robust control synthesis provides the powerful framework for handling various types of those uncertain dynamical RO plants. In this framework, $H_\infty$ loop shaping proposed by McFarlane and Glover [11] has proved itself to be an efficient control algorithm. However, the designed controllers often have high order and have not been applied in practice for RO plant control. In this paper, the system designers can apply simple PID control scheme incorporating the $H_\infty$ loop shaping framework to overcome those problems. The objective is to achieve a unique controller which has fixed structure and low order while retaining the stability and robustness against perturbed RO plants. Even the control design procedure follows $H_\infty$ loop shaping or very sophisticated control paradigm, the final controller is simply a PID methodology for MIMO desalination plants. Extensive simulation results demonstrate that the proposed control approach is numerically efficient and leads to clear system performance superior to those of conventional methods. Finally, this robust control approach provides a systematic quality water treatment for the uncertain RO dynamical systems.

## 2. System identification

Since the control performance of the closed-loop system depends on perfect controller tuning which needs a model-based algorithm, an accurate transfer function of the RO system is usually required. Some researchers have presented the RO transfer function based on real desalination plants. Alatiqi et al. [6] proposed a MIMO structure of RO plant in Doha from experiments in which the manipulated variables are pH and feed pressure, and the membrane is hollow fine fiber type. The control variables are chosen as permeate flux and salinity, which are fundamental in RO desalination monitoring. In this model, pH-value has no effect on water flux, while the feed pressure affects both outputs. So far many works on controlling RO plant have been carried out based on this model. However, the current common configuration used in desalination plants is composite polyamide spiral wound membrane. The composite membranes are chemically and physically stable even under a wide range of feed pH and display a strong resistance to bacterial degradation. In addition, they do not hydrolyze and are usually less influenced by membrane

compaction. They have an improved chemical resistance and a great tolerance against flow impurities. Besides they are durable and easy to clean [1]. Chaaben et al. [12] identified multivariable RO desalination process in the form of a transfer function matrix, including parameter variations. The mathematical model was formulated based on a solution-diffusion (SD) flow through a polyamide spiral wound membrane. Two manipulated variables in this model are pump speed and reject valve aperture. By choosing these manipulated variables, the product water flow and salinity are directly controlled for RO plants, which do not exploit the pH-value in pretreatment part.

### 2.1. Mathematical formulation

As illustrated in Fig. 1, the RO unit is described using SD model. This model was proposed by Lonsdale et al. [13], which is based on diffusion of the solvent (water) and solute (salt) through a polyamide spiral wound membrane. The following assumptions are firstly made to derive the mathematical model:

(1) The RO membrane has a homogeneous, and nonporous surface layer.
(2) Both the solvent and solute dissolve in this layer and then diffuse across it.
(3) The solute and solvent diffusion is uncoupled due to its own chemical potential gradient across the membrane.
(4) These gradients are the result of concentration and pressure differences across the membrane.
(5) The water density is a constant at all of the boundaries in each control volume of feed, permeate and concentrate side.

In this model, the pure water flux across the membrane is given by:

$$J_w = K_w(\Delta P - \Delta\pi) \tag{1}$$

where $K_w$ is the water permeability coefficient, $\Delta P$ the average pressure drop over the membrane and $\Delta\pi$ the osmotic pressure. They are calculated, respectively, as follows:

$$\Delta P = \frac{P_f + P_c}{2} - P_p \tag{2}$$

$$\Delta\pi = 2RT_o\left(\frac{S_f + S_c}{2} - S_p\right) \tag{3}$$

where $P$ is the pressure, $S$ the salinity, $R$ the gas constant, $T_o$ the temperature. In this case, $T_o$ is chosen as constant at 25°C. The subscript f indicates feed side, the subscript p indicates permeate side and subscript c refers to concentrate side (see Fig. 1).

The salt flux across the membrane is given by:

$$J_s = K_s(f_{cp}S_f - S_p) \tag{4}$$

where $K_s$ is the salt permeability coefficient, and $f_{cp}$ describes the concentration polarization factor. Then the product water flux is the sum of pure water flux and salt flux:

$$J_p = J_w + J_s \tag{5}$$

Finally, the product water flow through the membrane is given by the multiplication of water flux and membrane area:

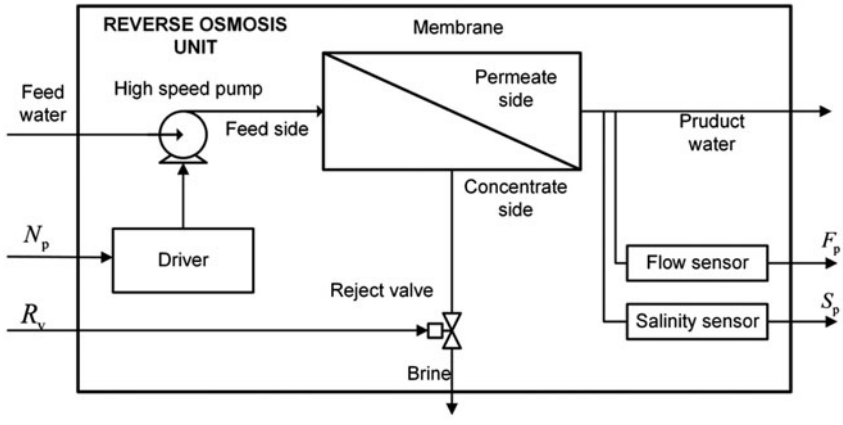


Fig. 1. Simplified model for RO process unit.

$$F_p = A_m J_p = A_m(J_w + J_s) \tag{6}$$

With having the fluxes of the related components, the following formulations are to identify the physical relations between input variables (pump speed and reject valve aperture) and outputs variables (product water flow and salinity). Substituting Eqs. (1) and (2) into Eq. (6) yields:

$$F_p = A_m\left[K_w\left(\frac{P_f + P_c}{2} - P_p - \Delta\pi\right) + J_s\right] \tag{7}$$

Using the fact in [12] that $P_f = K_p N_p^2$, the relation of pump speed $N_p$ and product water flow $F_P$ is described by:

$$F_p = A_m\left[K_w\left(\frac{K_p N_p^2 + P_c}{2} - P_p - \Delta\pi\right) + J_s\right] \tag{8}$$

where $K_p$ is the pump constant.

From Eq. (4), the product water salinity can be calculated by:

$$S_p = \frac{K_s f_{cp} S_f - J_s}{K_s} = f_{cp} S_f - \frac{F_f - F_w - F_c}{K_s A_m} \tag{9}$$

where $J_s = \frac{F_s}{A_m} = \frac{F_f - F_w - F_c}{A_m}$.

Providing that feed water salinity is fixed, it can be noted from Eq. (9) that the product water salinity is affected by the flow rates of the feed side $F_f$, the pure water $F_w$ and the concentrate side $F_c$, which are calculated, respectively, below.

The feed flow rate is given by [14]:

$$F_f = DN_p - c_s\frac{D}{2\pi}\frac{\Delta p}{\lambda} - F_r \tag{10}$$

where $D$ is the pump volumetric displacement per revolution, $c_s$ the pump slip coefficient, $\Delta p$ the pressure difference across the pump, $\lambda$ dynamic viscosity of feed water, $F_r$ the flow loss due to inlet flow restriction.

In addition, the pure water and the concentrate flow rate are expressed by:

$$F_w = J_w A_m \tag{11}$$

$$F_c = A_c^p v_c \tag{12}$$

According to Bartman et al. [15], the concentrate stream velocity $v_c$, (and in turn, the concentrate flow rate $F_c$) is affected by reject valve aperture $R_v$ given as follows:

$$\frac{dv_c}{dt} = \frac{A_f^p A_c^p}{A_m K_m V}(v_f - v_c) + \frac{A_c^p}{\rho V}\Delta\pi - \frac{1}{2}\frac{A_c^p r_c v_c^2}{V} \tag{13}$$

$$R_v = \mu \ln r_c + \phi \tag{14}$$

where $A^P$ is the cross-sectional area of the pipe, $K_m$ the overall feed side mass transfer coefficient, $V$ the system internal volume, $v$ the stream velocity, $\rho$ the feed water density, $r_c$ the reject valve resistance, $\mu$ and $\phi$ the reject valve constants. All the aforementioned equations show that there exist mutual relations between the process variables, where the pump speed $N_p$ and reject valve aperture $R_v$ have their effects on both product water flow $F_p$ and product water salinity $S_p$. The RO system model consists of a set of differential and algebraic equations and has to be solved simultaneously using computer-aided solver.

### 2.2. RO System model

Since the current market for RO membranes focus on thin-film composite polyamide type, the design objective in this study is to robustly control a small size RO unit using the model defined by Chaaben et al. [12]. This MIMO RO unit includes a high speed pump, a reject valve, a water flow sensor, a salinity sensor, and a polyamide-type membrane. The simplified block diagram of the RO desalination unit is depicted in Fig. 1. At a pump speed of 1,080 rpm and reject valve aperture of 50%, nominal water treatment capacity of the unit is 150 L/h in product water flow and 180 mg/L in product water salinity.

The output variables are product flow $F_p$ and product water salinity $S_p$. These two parameters are fundamental to control water quality and quantity in the desalination plants. This study focuses on designing the control system using two manipulated variables as pump speed $N_p$ and reject valve aperture $R_v$. Therefore, the simplified model given in Fig. 1 does not include the pre-treatment, pos-treatment systems and energy recovery device, which generally exist in modern RO plants.

As stated above, most physical systems including RO desalination plants are described in a set of partial differential equations, especially, they can be of high order in nature. However, these higher order equations only describe non-fundamental phenomena,

which can be reduced to more fundamental ones or simplified models, while fundamental physical equations are remarkably described in at most first or second order. In this paper, those neglected (higher-order) dynamics can be considered using the perturbed RO unit model in the robust control synthesis.

The RO unit model can be represented by the following transfer function [12]:

$$G(s) = \frac{Y(s)}{U(s)} = \begin{bmatrix} G_{11} = \frac{k_1}{\tau_1 s + 1} & G_{12} = \frac{-0.265\omega_{n1}^2}{s^2 + 2\xi_1\omega_{n1}s + \omega_{n1}^2} \\ G_{21} = \frac{-0.185\omega_{n2}^2}{s^2 + 2\xi_2\omega_{n2}s + \omega_{n2}^2} & G_{22} = \frac{k_2}{\tau_2 s + 1} \end{bmatrix} \tag{15}$$

where the control vector $U$, and output vector $Y$ are defined as:

$$U = \begin{bmatrix} N_p \\ R_v \end{bmatrix}, \quad Y = \begin{bmatrix} F_p \\ S_p \end{bmatrix} \tag{16}$$

In this paper, the transfer functions have been obtained using the system identification procedure based on the recursive least square with MATLAB software, which is provided by experimental input and output values. Specially, the first-order model is used for pump angular speed to product flow and reject valve aperture to product water salinity. Similarly, the second-order model is employed for reject valve aperture to product flow and pump angular speed to product water salinity.

By calculating the average values of the parameter variations, the constant gains are given as follows to generate a nominal model without uncertainty: $k_1 = 2.75$ and $k_2 = -0.18$; the time constants $\tau_1 = \tau_2 = 1.05$ (s); the natural frequencies $\omega_{n1} = 1.35$ (rad/s) and $\omega_{n2} = 1.935$ (rad/s); the damping ratios $\xi_1 = 0.4$ and $\xi_2 = 0.6$. These parametric values will be changed in some ranges from the nominal values to test the system performance of the designed controller for practical RO plants.

From the system transfer function in Eq. (15), the minimal state-space realization is calculated as follows:

$$G(s) = \left[\begin{array}{c|c} A_G & B_G \\ \hline C_G & D_G \end{array}\right] \tag{17}$$

where the state matrices are defined as:

$$A_G = \begin{bmatrix} -\frac{1}{\tau_1} & 1 & 0 & 0 \\ -\omega_{n1}^2 & -2\xi_1\omega_{n1} & 0 & 0 \\ 0 & 0 & -\frac{1}{\tau_2} & 1 \\ 0 & 0 & -\omega_{n2}^2 & -2\xi_2\omega_{n2} \end{bmatrix}$$

$$B_G = \begin{bmatrix} \frac{k_1}{\tau_1} & 0 \\ 0 & -0.265\omega_{n1}^2 \\ 0 & \frac{k_2}{\tau_2} \\ -0.185\omega_{n2}^2 & 0 \end{bmatrix}, C_G = \begin{bmatrix} 1 & 0 & 0 & 0 \\ 0 & 0 & 1 & 0 \end{bmatrix}, D_G = \begin{bmatrix} 0 & 0 \\ 0 & 0 \end{bmatrix} \tag{18}$$

## 3. Robust control synthesis

At first the minimal state-space of the modified PID structure is realized. Then the realization is embedded into the $H_\infty$ loop shaping framework in a two-degree of freedom configuration to enhance the controller performance (see Figs. 2 and 3). The shaped loop is accomplished by multiplying the nominal model with the compensators. This shaped loop can also be expressed under the form of normalized coprime factors, which allow the designers to create an uncertain plant by using coprime factor uncertainty description (see Fig. 4). Finally, based on the state-space representation of relevant matrices, the optimization problem to design the $H_\infty$ loop shaping with PID controller is solved using Schur bilinear matrix inequality. The robust controller is successfully designed if it can deal with parameter variations in the RO plants and provides the desired abilities of disturbance and noise rejections.

### 3.1. Modified PID control structure

The PID algorithm for the $H_\infty$ loop shaping framework is described as follows:

$$K_{PID_{ij}}(s) = k_{P_{ij}} + k_{I_{ij}}\frac{1}{s} + k_{D_{ij}}\frac{s}{\tau s + 1} \tag{19}$$

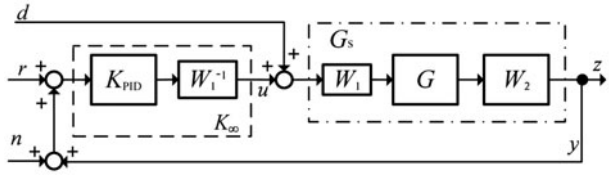


Fig. 2. $H_\infty$ loop shaping setup for tuning PID design parameters.

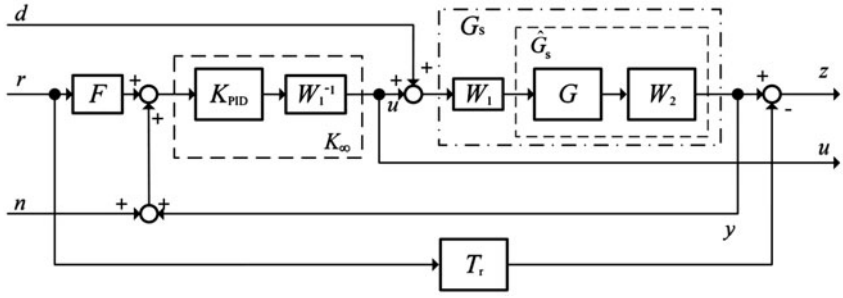


Fig. 3. New $H_\infty$ robust control formulation.

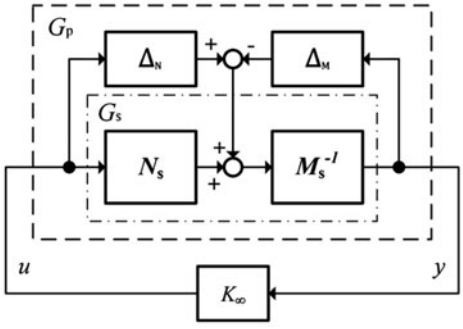


Fig. 4. Closed-loop control system with coprime plant perturbation.

where $K_{PIDij}(s)$ is the ijth element of the transfer function matrix $K_{PID}(s)$, $k_{Pij}$ is the ijth element of the proportional gains, $k_{I_{ij}}$ is the ijth element of the integral gains, $k_{Dij}$ is the ijth element of the derivative gains, and $\tau$ is the derivative action time constant.

The control algorithm in Eq. (19) can be rewritten as:

$$K_{PID_{ij}}(s) = \frac{\left(k_{I_{ij}}\tau - \frac{k_{D_{ij}}}{\tau}\right)s + k_{I_{ij}}}{\tau s^2 + s} + k_{P_{ij}} + \frac{k_{D_{ij}}}{\tau} = \frac{K_{D_{ij}}s + K_{I_{ij}}}{\tau s^2 + s} + K_{P_{ij}} \quad (20)$$

where $K_{P_{ij}} = k_{P_{ij}} + k_{D_{ij}}/\tau$, $K_{I_{ij}} = k_{I_{ij}}$, and $K_{D_{ij}} = k_{I_{ij}}\tau - k_{D_{ij}}/\tau$.

Hence, the PID control structure for the RO unit with two inputs and two outputs become:

$$K_{PID}(s) = \begin{bmatrix} \frac{K_{D_{11}}s + K_{I_{11}}}{\tau s^2 + s} + K_{P_{11}} & \frac{K_{D_{12}}s + K_{I_{12}}}{\tau s^2 + s} + K_{P_{12}} \\ \frac{K_{D_{21}}s + K_{I_{21}}}{\tau s^2 + s} + K_{P_{21}} & \frac{K_{D_{22}}s + K_{I_{22}}}{\tau s^2 + s} + K_{P_{22}} \end{bmatrix} \quad (21)$$

Let $\eta = 1/\tau$, then a partial fraction expansion of $K_{PID}(s)$ is derived as follows:

$$K_{PID}(s) = D_K + \frac{B_{K1}}{s} + \frac{B_{K2}}{s + \eta} \quad (22)$$

where

$$D_K = K_P = \begin{bmatrix} k_{P_{11}} + \eta k_{D_{11}} & k_{P_{12}} + \eta k_{D_{12}} \\ k_{P_{21}} + \eta k_{D_{21}} & k_{P_{22}} + \eta k_{D_{22}} \end{bmatrix} \quad (23)$$

$$B_{K1} = K_I = \begin{bmatrix} k_{I_{11}} & k_{I_{12}} \\ k_{I_{21}} & k_{I_{22}} \end{bmatrix} \quad (24)$$

$$B_{K2} = K_D - \frac{K_I}{\eta} = \begin{bmatrix} -\eta^2 k_{D_{11}} & -\eta^2 k_{D_{12}} \\ -\eta^2 k_{D_{21}} & -\eta^2 k_{D_{22}} \end{bmatrix} \quad (25)$$

Finally, from partial fraction expansion in Eq. (22), the minimal state-space realization of $K_{PID}(s)$ can be formulated as follows:

$$K_{PID}(s) = \left[\begin{array}{cc|c} 0 & 0 & B_{K1} \\ 0 & -\eta I & B_{K2} \\ \hline I & I & D_K \end{array}\right] = \left[\begin{array}{c|c} A_K & B_K \\ \hline C_K & D_K \end{array}\right] \quad (26)$$

### 3.2. PID controller in the $H_\infty$ loop shaping design

The $H_\infty$ loop shaping framework proposed by McFarlane and Glover [11] offers a computationally efficient method to design robust controllers. In the framework, the system designer shapes the open-loop plant $G$ with the pre-compensator $W_1$ and post-compensator $W_2$ as shown in Fig. 2 to obtain the shaped loop plant $G_s$ with desired loop gains at specified frequencies. Typically, the loop gains have to be large at low frequencies for good disturbance rejection at both the input and the output of the plant, and small at high frequencies for noise rejection. In addition, the desired open loop shapes are chosen to be approximately −20 dB/decade roll-off around the

crossover frequency to achieve robust stability, gain, and phase margins.

Using the method proposed by Genc [16], the structure of controller $K_\infty$ in Fig. 2 is given as:

$$K_\infty = W_1^{-1} K_{\mathrm{PID}} \tag{27}$$

Hence, the final controller $K$ has the desired PID structure as follows:

$$K = W_1 K_\infty W_2 = K_{\mathrm{PID}} W_2 \tag{28}$$

However, the control configuration of Genc [16] has only one degree of freedom, which is not sufficient to meet both time-domain constraints and robust gain margin for the frequency domain. As illustrated in Fig. 3, a two-degree of freedom strategy is designed including feedback controller $K_\infty$ and set-point filtering structure $F$. The set-point filter $F$ only effects on the reference signal to improve settling time while decrease overshoot and the interactions between channels. The filter has been designed to guarantee that the performance of the feedback system matches as closely as possible that of the reference model $T_r$. In this new formation, $W_1$ and $W_1^{-1}$ only affect the closed-loop system indirectly though $K_{\mathrm{PID}}$ since $K_{\mathrm{PID}}$ is formed with respect to the shaped plant $G_s$ that includes the compensators of $W_1$ and $W_2$.

The optimization problem is to minimize the $H_\infty$ norm of the transfer function matrix $T$ from the disturbance $d$, the reference $r$ and the noise $n$ to the regulated output $z$ and the control effort $u$ by designing the controller $K_{\mathrm{PID}}$ and the filter $F$ to obtain a desired value $\gamma$ as follows:

$$\gamma \geq \left\| T \begin{bmatrix} d \\ r \\ n \end{bmatrix} \to \begin{bmatrix} z \\ u \end{bmatrix} \right\|_\infty = \left\| \begin{bmatrix} G_s & (I - W_2 G K_{\mathrm{PID}})^{-1} W_2 G K_{\mathrm{PID}} F - T_r & (I - W_2 G K_{\mathrm{PID}})^{-1} W_2 G K_{\mathrm{PID}} \\ (I - K_{\mathrm{PID}} W_2 G)^{-1} W_1^{-1} K_{\mathrm{PID}} G_s & W_1^{-1} K_{\mathrm{PID}} F & K_{\mathrm{PID}} \end{bmatrix} \right\|_\infty = \left\| \begin{bmatrix} \hat{G}_s W_1 & (I - \hat{G}_s K_{\mathrm{PID}})^{-1} \hat{G}_s K_{\mathrm{PID}} F - T_r & (I - \hat{G}_s K_{\mathrm{PID}})^{-1} \hat{G}_s K_{\mathrm{PID}} \\ (I - K_{\mathrm{PID}} \hat{G}_s)^{-1} W_1^{-1} K_{\mathrm{PID}} \hat{G}_s W_1 & W_1^{-1} K_{\mathrm{PID}} F & K_{\mathrm{PID}} \end{bmatrix} \right\|_\infty \tag{29}$$

where

$$\hat{G}_s = W_2 G \tag{30}$$

$$G_s = W_2 G W_1 = M_s^{-1} N_s \tag{31}$$

Note that $G_s$ is the shaped loop plant, $M_s$ and $N_s$ are nominator and denominator normalized coprime factors as described in Eq. (32) and Fig. 4.

The robust stabilization problem is to stabilize the set of following perturbed plants:

$$G_p(s) = (M_s + \Delta_M)^{-1}(N_s + \Delta_N), \quad \|[\Delta_N - \Delta_M]\|_\infty \leq \varepsilon \tag{32}$$

where $\Delta_M$ and $\Delta_N$ denote uncertainties in nominator and denominator factors to create the uncertain system $G_p$.

The inverse of $\gamma$ is the so-called robust stability margin $\varepsilon$, or $= 1/\gamma$ which is the indicator of the achieved robust stability of the shaped loop. For practical implementation, the stability margin $\varepsilon > 0.25$ is acceptable. In turn, the compensated system will satisfy both robust stability and robust performance simultaneously.

It is noted that the uncertainty model in $H_\infty$ loop shaping algorithm is the coprime factor uncertainty (see Fig. 4). This uncertainty description is general and has distinct advantages over the other approaches. It is possible to represent a greater variety of the system uncertainties and no priori uncertainty information is needed. Indeed it captures all low and high frequency perturbations, unmodeled dynamics and parameter variations in the RO desalination plants. Thus, the obtained controller will robustly stabilize the perturbed plant against a very general uncertainty.

### 3.3. Solving optimization

The optimization problem in Eq. (29) is solved using a bilinear matrix inequality based on state-space realization of the relevant matrices. A minimal state-space realization for the transfer matrix $T$ is obtained as follows:

$$T_{\begin{bmatrix} d \\ r \\ n \end{bmatrix} \to \begin{bmatrix} z \\ u \end{bmatrix}} = \left[\begin{array}{c|c} A_{\mathrm{T}} & B_{\mathrm{T}} \\ \hline C_{\mathrm{T}} & D_{\mathrm{T}} \end{array}\right]$$

$$= \left[\begin{array}{cccccc|ccc} A_{\mathrm{i}} & 0 & B_{\mathrm{i}}C_{\mathrm{K}} & B_{\mathrm{i}}D_{\mathrm{K}}C_{\mathrm{F}} & 0 & B_{\mathrm{i}}D_{\mathrm{K}}C & 0 & B_{\mathrm{i}}D_{\mathrm{K}}D_{\mathrm{F}} & B_{\mathrm{i}}D_{\mathrm{K}} \\ 0 & A_{\mathrm{l}} & 0 & 0 & 0 & 0 & B_{\mathrm{l}} & 0 & 0 \\ 0 & 0 & A_{\mathrm{K}} & B_{\mathrm{K}}C_{\mathrm{F}} & 0 & B_{\mathrm{K}}C & 0 & B_{\mathrm{K}}D_{\mathrm{F}} & B_{\mathrm{K}} \\ 0 & 0 & 0 & A_{\mathrm{F}} & 0 & 0 & 0 & B_{\mathrm{F}} & 0 \\ 0 & 0 & 0 & 0 & A_{\mathrm{Tr}} & 0 & 0 & B_{\mathrm{Tr}} & 0 \\ 0 & BC_{\mathrm{l}} & BC_{\mathrm{K}} & BD_{\mathrm{K}}C_{\mathrm{F}} & 0 & A+BD_{\mathrm{K}}C & BD_{\mathrm{l}} & BD_{\mathrm{K}}D_{\mathrm{F}} & BD_{\mathrm{K}} \\ \hline C_{\mathrm{i}} & 0 & D_{\mathrm{i}}C_{\mathrm{K}} & D_{\mathrm{i}}D_{\mathrm{K}}C_{\mathrm{F}} & 0 & D_{\mathrm{i}}D_{\mathrm{K}}C & 0 & D_{\mathrm{i}}D_{\mathrm{K}}D_{\mathrm{F}} & D_{\mathrm{i}}D_{\mathrm{K}} \\ 0 & 0 & 0 & 0 & -C_{\mathrm{Tr}} & C & 0 & -D_{\mathrm{Tr}} & 0 \end{array}\right] \tag{33}$$

where the state-space realizations of the related transfer functions are given by:

$$\hat{G}_{\mathrm{s}}(s) = W_2 G = \left[\begin{array}{c|c} A & B \\ \hline C & D \end{array}\right] \tag{34}$$

$$W_{\mathrm{l}}(s) = \left[\begin{array}{c|c} A_{\mathrm{l}} & B_{\mathrm{l}} \\ \hline C_{\mathrm{l}} & D_{\mathrm{l}} \end{array}\right] \tag{35}$$

$$W_{\mathrm{l}}^{-1}(s) = \left[\begin{array}{c|c} A_{\mathrm{i}} & B_{\mathrm{i}} \\ \hline C_{\mathrm{i}} & D_{\mathrm{i}} \end{array}\right] \tag{36}$$

$$F(s) = \left[\begin{array}{c|c} A_{\mathrm{F}} & B_{\mathrm{F}} \\ \hline C_{\mathrm{F}} & D_{\mathrm{F}} \end{array}\right] \tag{37}$$

$$T_{\mathrm{r}}(s) = \left[\begin{array}{c|c} A_{\mathrm{Tr}} & B_{\mathrm{Tr}} \\ \hline C_{\mathrm{Tr}} & D_{\mathrm{Tr}} \end{array}\right] \tag{38}$$

According to the Bounded real lemma for any $\gamma > 0$, the condition $\|T\|_\infty$ in Eq. (29) holds if and only if there exists a symmetric positive definite matrix $X$ such that:

$$\begin{pmatrix} A_{\mathrm{T}}^T X + X A_{\mathrm{T}} + C_{\mathrm{T}}^T C_{\mathrm{T}} & X B_{\mathrm{T}} + C_{\mathrm{T}}^T D_{\mathrm{T}} \\ B_{\mathrm{T}}^T X + D_{\mathrm{T}}^T C_{\mathrm{T}} & D_{\mathrm{T}}^T D_{\mathrm{T}} - \gamma^2 I \end{pmatrix} < 0 \tag{39}$$

Then Eq. (39) is rearranged as follows:

$$\begin{pmatrix} X A_{\mathrm{T}} + A_{\mathrm{T}}^T X & X B_{\mathrm{T}} \\ B_{\mathrm{T}}^T X & -\gamma^2 I \end{pmatrix} + \begin{pmatrix} C_{\mathrm{T}}^T \\ D_{\mathrm{T}}^T \end{pmatrix} I \begin{pmatrix} C_{\mathrm{T}} & D_{\mathrm{T}} \end{pmatrix} < 0 \tag{40}$$

Let $P_{\mathrm{L}} = \gamma^{-1} X$ and multiply Eq. (40) by $\gamma^{-1}$ to get the form of Schur complement formula as follows:

$$\begin{pmatrix} P_{\mathrm{L}} A_{\mathrm{T}} + A_{\mathrm{T}}^T P_{\mathrm{L}} & P_{\mathrm{L}} B_{\mathrm{T}} \\ B_{\mathrm{T}}^T P_{\mathrm{L}} & -\gamma I \end{pmatrix} + \begin{pmatrix} C_{\mathrm{T}}^T \\ D_{\mathrm{T}}^T \end{pmatrix} \gamma^{-1} I \begin{pmatrix} C_{\mathrm{T}} & D_{\mathrm{T}} \end{pmatrix} < 0 \tag{41}$$

Finally, the optimization problem in Eq. (29) can be written in the equivalent form of Schur complement formula as:

min $\gamma(P_{\mathrm{L}}, A_{\mathrm{K}}, B_{\mathrm{K}}, C_{\mathrm{K}}, D_{\mathrm{K}}, A_{\mathrm{F}}, B_{\mathrm{F}}, C_{\mathrm{F}}, D_{\mathrm{F}})$ such that:

$$\begin{pmatrix} P_{\mathrm{L}} A_{\mathrm{T}} + A_{\mathrm{T}}^{\mathrm{T}} P_{\mathrm{L}} & P_{\mathrm{L}} B_{\mathrm{T}} & C_{\mathrm{T}}^{\mathrm{T}} \\ B_{\mathrm{T}}^{\mathrm{T}} P_{\mathrm{L}} & -\gamma I & D_{\mathrm{T}}^{\mathrm{T}} \\ C_{\mathrm{T}} & D_{\mathrm{T}} & -\gamma I \end{pmatrix} < 0, \quad P_{\mathrm{L}} > 0 \tag{42}$$

where the symmetric positive matrix $P_{\mathrm{L}}$ is the Lyapunov function matrix.

Table 1
Model parameters variations

| Parameters | Min. values | Ave. values | Max. values | Unit |
|---|---|---|---|---|
| $k_1$ | 1.13 | 2.75 | 4.37 | Unitless |
| $\tau_1$ | 0.43 | 1.05 | 1.67 | s |
| $k_2$ | −0.29 | −0.18 | −0.07 | Unitless |
| $\tau_2$ | 0.43 | 1.05 | 1.67 | s |
| $\omega_{n1}$ | 0.55 | 1.35 | 2.15 | Rad/s |
| $\zeta_1$ | 0.16 | 0.4 | 0.64 | Unitless |
| $\omega_{n2}$ | 0.79 | 1.935 | 3.08 | Rad/s |
| $\zeta_2$ | 0.25 | 0.6 | 0.95 | Unitless |

This is a bilinear matrix inequality optimization problem. The local optimal solution is found through alternately minimizing the optimal cost $\gamma$ with respect to $P_L$ with controller parameters fixed and vice versa [16].

## 4. Simulation setup

As mentioned before, the membrane in RO process unit is very sensitive to the changes in temperature, feed water salinity, fouling, and many other factors. In this simulation, only feed water salinity change is considered to be the source of parametric uncertainties. If the feed water salinity varies, the parameters of the transfer function $G(s)$ in Eq. (15) are supposed to vary in the intervals as shown in Table 1. These parameter variations are up to ±59% of the nominal values and they are chosen to test the controller performance. The parametric uncertainties assumed are much larger than those in [12] and will cause larger plant-model mismatch. The robust controller has been successfully designed if it can handle those variations and has desired abilities of disturbance rejection and noise attenuation.

Besides the set of parametric uncertainties, the system designers also introduce disturbances at the system outputs and noise signals at the feedback of the closed-loop system to confirm controller's performance. The closed-loop system has been tested for robust stability and performance under given simulation conditions.

## 5. Results and discussion

Insuring drinking water of acceptable quality is very important to the success of the RO desalination plants. Beside the external factors, the product water flow also affects the salinity, which is the water quality of the output. Moreover, the turbulent feed flow created by high speed pump can reduce concentration polarization, leading to reduced fouling and scaling. On the contrary, a higher permeate flux increases the concentration polarization [3]. Therefore, pump speed, product water flow and salinity are strictly required to be stable at all times against uncertainties and disturbances. The product water also needs to reach desired values in short time with small overshoot, and the dynamic couplings between control channels are minimized.

Then the performance requirements of the desalination control system are selected as follows:

(1) The stability margin is $\varepsilon > 0.3$.
(2) The effects of external disturbances and measurement noises are reduced at least 30%.
(3) The time-domain transient responses have settling times less than 5s, overshoots less than 10%, and zero steady-state errors.
(4) The control interactions between channels are less than 20% during rising time.

The state-space representations of the reference system $T_r$, compensators $W_1$ and $W_2$ that enable the system designer to achieve the desired loop shape are chosen respectively as follows:

$$A_{Tr} = \begin{bmatrix} -1 & 0 \\ 0 & -1.35 \end{bmatrix}, \quad B_{Tr} = \begin{bmatrix} 1 & 0 \\ 0 & 1 \end{bmatrix}$$
$$C_{Tr} = \begin{bmatrix} 1 & 0 \\ 0 & 1 \end{bmatrix}, \quad D_{Tr} = \begin{bmatrix} 0 & 0 \\ 0 & 0 \end{bmatrix} \tag{43}$$

$$A_1 = \begin{bmatrix} -1.10^{-3} & 0 \\ 0 & -1.10^{-3} \end{bmatrix}, \quad B_1 = \begin{bmatrix} 1 & 0 \\ 0 & 2 \end{bmatrix}$$
$$C_1 = \begin{bmatrix} 1.19 & 0 \\ 0 & 2.09 \end{bmatrix}, \quad D_1 = \begin{bmatrix} 1 & 0 \\ 0 & 2.8 \end{bmatrix} \tag{44}$$

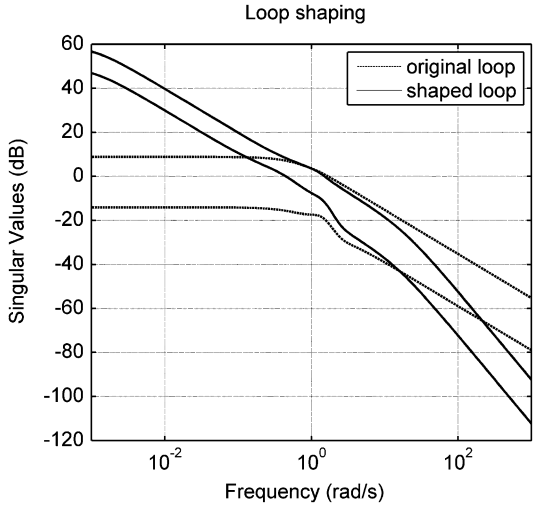


Fig. 5. Frequency responses of the original and shaped loop.

$$A_2 = \begin{bmatrix} -28 & 0 \\ 0 & -16 \end{bmatrix}, \quad B_2 = \begin{bmatrix} 4 & 0 \\ 0 & 4 \end{bmatrix}$$
$$C_2 = \begin{bmatrix} 6.5 & 0 \\ 0 & 7 \end{bmatrix}, \quad D_2 = \begin{bmatrix} 0 & 0 \\ 0 & 0 \end{bmatrix} \tag{45}$$

The frequency response curves of the shaped loop relating to original loop are shown in Fig. 5. It can be observed that the shaped loop has high gain at low frequency and low gain at high frequency as desired.

Based on the shaped loop and reference system $T_r$, a four-state filter $F$ and a six-order $H_\infty$ loop shaping PID controller have been synthesized. The achieved value of  is approximately 0.59. This indicates good stability margin, and 59% of coprime factor uncertainties is allowed around the crossover frequency. It is noted that the designed controller can successfully handle the parametric variations proposed in Table 1. The detailed controller parameters are given as follows:

$$A_K = \begin{bmatrix} 0 & 0 & 0 & 0 \\ 0 & 0 & 0 & 0 \\ 0 & 0 & -1.55 & 0 \\ 0 & 0 & 0 & -1.55 \end{bmatrix}, \quad B_K = \begin{bmatrix} 1 & 0 \\ 0 & 1 \\ 1.55 & 0 \\ 0 & 1.55 \end{bmatrix}$$
$$C_K = \begin{bmatrix} -0.92 & 0.37 & 0.26 & 0.47 \\ 1.59 & 3.28 & -1.35 & -0.64 \end{bmatrix}, \quad D_K = \begin{bmatrix} -1.16 & 0.19 \\ 2.85 & 3.13 \end{bmatrix} \tag{46}$$

$$A_F = \begin{bmatrix} -1.87 & 0 & 0 & 0 \\ 0 & -1.12 & 0 & 0 \\ 0 & 0 & -0.77 & 0 \\ 0 & 0 & 0 & -0.87 \end{bmatrix}, \quad B_F = \begin{bmatrix} 1.87 & 0 \\ 0 & 1.12 \\ 0.77 & 0 \\ 0 & 0.87 \end{bmatrix}$$
$$C_F = \begin{bmatrix} 1 & -0.046 & 0 & 0 \\ 0 & 0 & -0.11 & 1 \end{bmatrix}, \quad D_F = \begin{bmatrix} 0 & 0.046 \\ 0.11 & 0 \end{bmatrix} \tag{47}$$

The step references of 150 L/h and 180 mg/L are set for the first and second channel, respectively. Figs. 6–8 show the performance of the closed-loop system with the $H_\infty$ loop shaping PID controller, in comparison with those of a conventional PID controller. The noise attenuation ability of a conventional PID controller is also plotted in Fig. 9 for better comparison. For the sake of clarity, three plant models have been selected to demonstrate the dynamic performance of the set of perturbed RO system controlled by the $H_\infty$ loop shaping PID controller: the nominal (nom) model with average parameters, the minimum (min) model with minimum parameters and maximum (max) model with maximum parameters in Table 1.

It can be seen from Fig. 6(a) and (d) that both performance outputs reach the reference targets in less than 4s with almost no overshoot in both channels, comparing to the same settling time but 10% overshoot in the first channel and 6s-settling time in the second channel for the conventional PID controller. It is also noted from Fig. 6(b) and (c) that the interactions between two channels are insignificant before going to zero in steady state, while the interactions are greater than 20% in case of the conventional PID controller. Note that a big overshoot can momentarily affect product water quality, and high mutual coupling can deeply deteriorate the system performance of MIMO plant. Furthermore, there are only slight differences among the transient responses of nominal, minimum and maximum model. It proves that the proposed controller overcomes modeling mismatch effectively, and the set of perturbed systems satisfies the control requirements.

The transient responses of the $H_\infty$ loop shaping PID controller show better than those of PI controller using optimization techniques [17]. Furthermore, this study sufficiently addresses the robustness issue of a RO control system under uncertainties, disturbances and noises.

In addition, the abilities of disturbances and noises attenuation are more likely to be important in verifying controller's performance. The disturbances can be

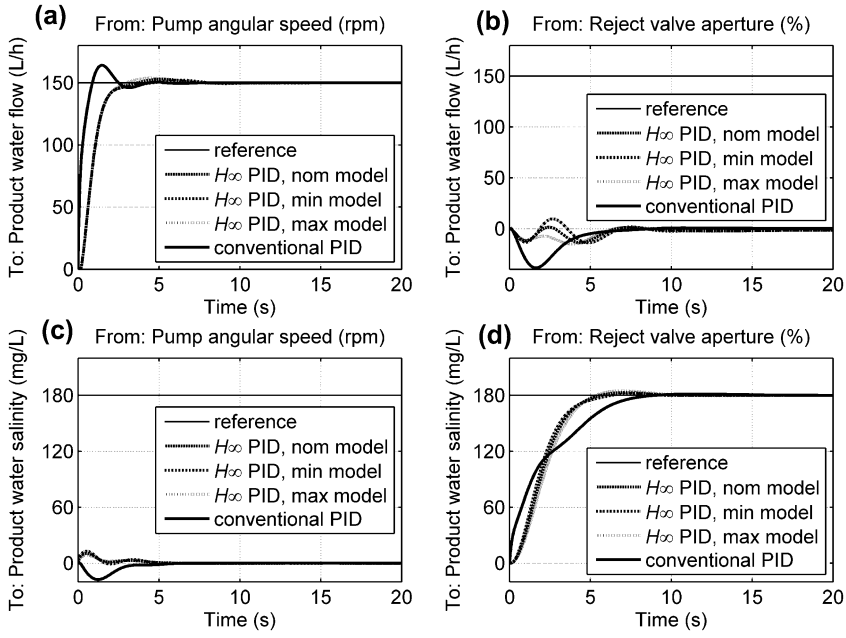


Fig. 6. Transient responses of RO systems with $H_\infty$ loop shaping PID and conventional PID controllers: (a) response of product water flow to pump angular speed, (b) response of product water flow to reject valve aperture, (c) response of product water salinity to pump angular speed and (d) response of product water salinity to reject valve aperture.

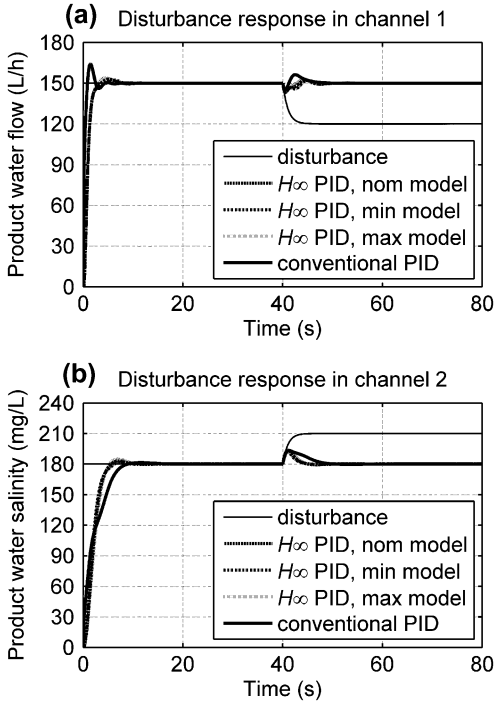


Fig. 7. Time history due to disturbances of RO systems with $H_\infty$ loop shaping PID controller and conventional PID controller: (a) response of product water flow to disturbances and (b) response of product water salinity to disturbances.

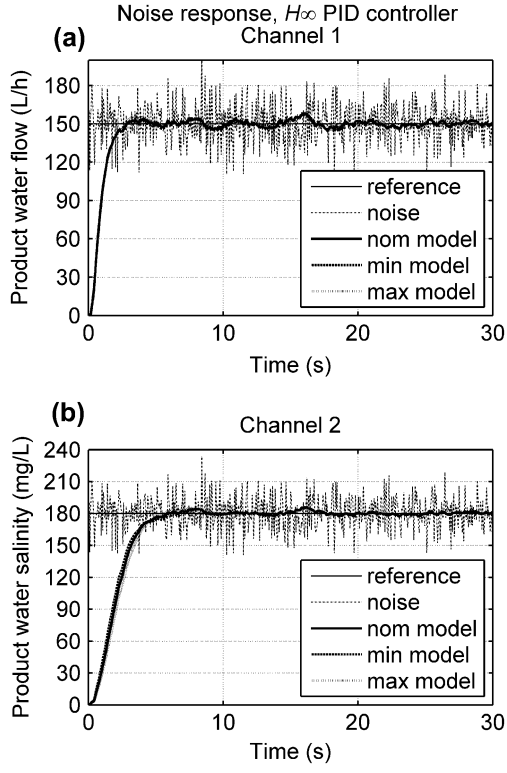


Fig. 8. Time history due to noises of RO systems with $H_\infty$ loop shaping PID controller: (a) response of product water flow to noise and (b) response of product water salinity to noise.

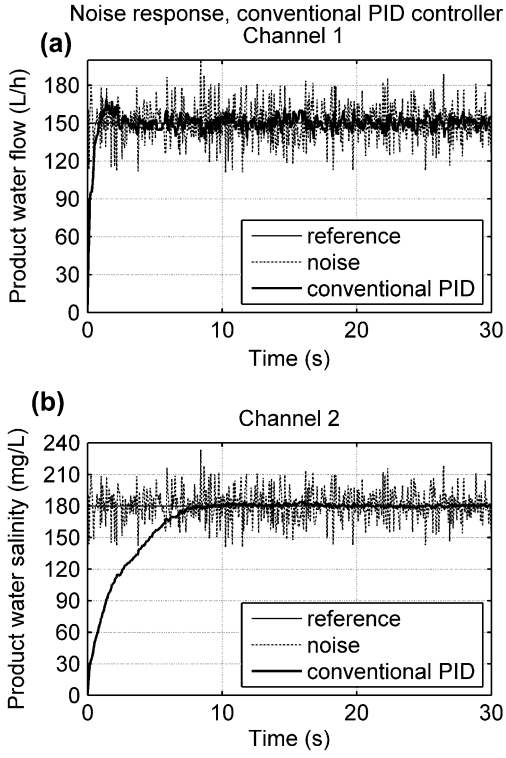


Fig. 9. Time history due to noises of RO system with conventional PID controller: (a) response of product water flow to noise and (b) response of product water salinity to noise.

the causes of leakage, air in the system or fouling, etc., while measurement noises are inherent to all electronic sensors.

According to Sangyoup et al. [18], colloidal fouling will cause significant decrease in the salt rejection ability of the membrane. The consequential effects are decrease in product water flow and increase in product water salinity. In this study, two disturbance inputs of −30 L/h and 30 mg/L have been applied to the first and second channel at 40th second, respectively. These disturbances represent a decrease in product water flow and an increase in product water salinity resulting from colloidal fouling, which need to be eliminated in a short time. As illustrated in Fig. 7(a) and (b), the external disturbances have been reduced up to 90% in the first channel and 60% in the second channel. Whenever there are no changes in the external disturbances, the errors will go to zero. Hence, the closed-loop system is stable even under large disturbances. While these disturbances occur faster than would usually occur in practice, the ability to eliminate them will insist on a controller that is also able to cope with slower disturbances. It can also be observed that closed-loop system with $H_\infty$ loop shaping PID controller is more stable than the conventional PID controller case.

In practice, the external disturbances are often described by low-frequency signals, whereas measurement noises are often high-frequency signals. Sensor noise is unavoidable and can cause some errors to the control system. Therefore, it is also necessary to eliminate noise effects on RO system. In addition, the input references with sensor noises have been applied to two channels. Fig. 8(a) and (b) shows the noise attenuation ability of the achieved controller in a high-frequency range. It can be observed that 70% of noises in the first channel and 90% in the second channel have been eliminated. From the magnitudes of noises and the changes in responses, one can conclude that the presented closed-loop system is unsusceptible to sensor noises. The noise sensitivity of the conventional PID controller is also illustrated in Fig. 9, where the first channel is deeply affected by the same noises. The performance comparison proves that the $H_\infty$ loop shaping PID controller can effectively eliminate measurement noises in the process. These characteristics will be utilized in practical implementation for controlling RO desalination plants.

In this paper, the performance of the control system has been assessed by measuring through product water flow and salinity. From the mathematical formulation, it is also noted that feed pressure is a mediate variable between inputs and outputs. Both manipulated variables have effects on feed pressure and this pressure affects both controlled variables. Our future study will be on nested control system, where inner loop is based on pressure controlling and outer one is based on product water flow and salinity controlling.

## 6. Conclusion

This paper presents a new approach to robust quality water control for RO desalination plants. The common controller to manage the RO dynamical system is PID control approach due to specific software and hardware installed in desalination plants. However, it is getting more difficult to control desalination plants against the model uncertainties, external disturbances and sensor noises to meet water quality requirements. Therefore, it is necessary to design a more powerful controller than the conventional one to better manage RO plants. This study has introduced a modified PID controller into the $H_\infty$ loop shaping framework. The design objectives are to simplify the controller structure, reduce the controller's order and

still retain the robust performance under various uncertainties and disturbances. The coprime factor uncertainty used in the methodology bounds great variety of the system uncertainties, and no priori uncertainty information is required, which is typically suitable for RO desalination plants. The achieved controller can be used for MIMO plants and has fixed structure with 6 orders. The simulation results show that the presented controller offers significant improvement in transient responses, high ability of decoupling, disturbance, and noise attenuation while still retaining the high robust stability margin of 59%. In other words, this robust controller can preserve high product water quality and flow of RO systems under large uncertainties, disturbances, and noises. Consequently, it will help increase productivity and prolong the life of the membranes, save energy, and lower product water costs. Since the proposed controller has both the simplicity and robustness characteristics, this can be effectively used for quality water treatment in the complicated RO desalination process.

**Nomenclature**

$A_m$ — membrane area ($m^2$)
$c_s$ — pump slip coefficient (Pa)
$d$ — input disturbance
$D$ — pump volumetric displacement per revolution (L/rev)
$f_{cp}$ — concentration polarization factor
$F$ — set-point filter
$F_p$ — product water flow (L/h)
$F_r$ — flow loss due to inlet flow restriction (L/h)
$G$ — nominal system
$G_p$ — perturbed plant
$G_s$ — shaped loop plant
$J$ — flux ($kg/m^2\ s^{-1}$)
$k$ — process gain
$k_P$ — proportional gain
$k_I$ — integral gain
$k_D$ — derivative gain
$K_m$ — overall feed-side mass transfer coefficient (m/s)
$K_{PID}$ — proportional-integral-derivative controller
$K_p$ — pump constant
$K_s$ — salt permeability coefficient ($m/s\ pa^{-1}$)
$K_w$ — water permeability coefficient ($m/s\ pa^{-1}$)
$M_s$, $N_s$ — normalized coprime factors
$n$ — noise
$N_p$ — angular pump speed (rpm)
$P$ — pressure
$P_L$ — Lyapunov function matrix
$r$ — reference input
$r_c$ — reject valve resistance
$R$ — gas constant
$R_v$ — reject brine valve aperture (%)
$s$ — Laplace variable
$S_p$ — product water salinity (mg/L)
$T$ — state-space realization from inputs to outputs
$T_o$ — temperature (°C)
$T_r$ — reference system
$u$ — control signal
$U$ — input vector
$v$ — stream velocity (m/s)
$V$ — internal volume of the system (L)
$W$ — weighting function
$Y$ — output vector
$z$ — regulated output vector

*Greek letters*

$\Delta_M$, $\Delta_N$ — uncertainty transfer functions
$\Delta p$ — pressure drop across the pump (Pa)
$\Delta\pi$ — osmotic pressure (Pa)
$\varepsilon$ — stability gain margin
$\gamma$ — optimal cost
$\lambda$ — dynamic viscosity of feed water (Pa/s)
$\varphi$, $\mu$ — reject valve constant
$\rho$ — feed water density ($kg/m^3$)
$\tau$ — derivative gain
$\omega_n$ — natural frequency (rad/s)
$\xi$ — damping coefficient

## References

[1] A. Rodríguez-Calvo, G.A. Silva-Castro, F. Osorio, J. González-López, C. Calvo, Reverse osmosis seawater desalination: Current status of membrane systems, Desalin. Water Treat. 56 (2015) 849–861.
[2] A. Gambier, A. Wellenreuther, E. Badreddin, Optimal control of a reverse osmosis desalination plant using multi-objective optimization, Proc. 2006 IEEE Conference on Control Applications, Munich, Germany, 4–6 October 2006.
[3] C.Z. Kolk, W. Hater, N. Kempken, Cleaning of reverse osmosis membranes, Desalin. Water Treat. 51 (2013) 343–351.
[4] S. Sobana, R.C. Panda, Identification, modelling, and control of continuous reverse osmosis desalination system: A review, Sep. Sci. Technol. 46 (2011) 551–560.
[5] A. Gambier, E. Badreddin, A robust control approach for a reverse osmosis desalination plant, powered by renewable energy sources, Proc. 12th Conference on Environmental Science and Technology CEST 2011, Rhodes, Greece, 8–10 September 2011.
[6] I. Alatiqi, A. Ghabris, S. Ebrahim, System identification and control of reverse osmosis desalination, Desalination 75 (1989) 119–140.
[7] G. Kim, J. Park, J. Kim, H. Lee, H. Heo, PID control of reverse osmosis desalination plant using immune-genetic algorithm, ICROS-SICE International Joint Conference, Fukuoka, Japan, 18–21 August 2009.
[8] N.S. Rathore, N. Kundariya, A. Narain, PID controller tuning in reverse osmosis system based on particle swarm optimization, Int. J. Sci. Res. Publ. 3 (2013) 1–5.

[9] N.S. Rathore, D.P.S. Chauhan, V.P. Singh, Luus-Jaakola optimization procedure for PID controller tuning in reverse osmosis system, Proc. 23rd IRF International Conference, Chennai, India, 2015, 12–15.
[10] K. Chithra, A. Srinivasan, V. Vijayalakshmi, A. Asuntha, PID controller tuning in reverse osmosis system based on particle swarm optimization, Int. J. Res. Appl. Sci. Eng. Technol. 3 (2015) 351–358.
[11] D. McFarlane, K. Glover, A loop-shaping design procedure using $H_\infty$ synthesis, IEEE Trans. Autom. Control 37 (1992) 759–769.
[12] A.B. Chaaben, R. Andoulsi, A. Sellami, R. Mhiri, MIMO modeling approach for a small photovoltaic reverse osmosis desalination system, J. Appl. Fluid Mech. 4 (2011) 35–41.
[13] H. Lonsdale, U. Merten, R. Riley, Transport properties of cellulose acetate osmotic membranes, J. Appl. Polym. Sci. 9 (1965) 1341–1362.
[14] A.M. Bilton, L.C. Kelley, S. Dubowsky, Photovoltaic reverse osmosis—Feasibility and a pathway to develop technology, Desalin. Water Treat. 31 (2011) 24–34.
[15] A.R. Bartman, P.D. Christofides, Y. Cohen, Nonlinear modeled-based control of an experimental reverse osmosis water desalination system, Ind. Eng. Chem. Res. 48 (2009) 6126–6136.
[16] A.U.Genc, A state-space algorithm for designing $H_\infty$ loop shaping PID controllers, Technical Report, Cambridge University, Cambridge, UK, October 2000.
[17] A. Gambier, A. Wellenreuther, E. Badreddin, Control system design of reverse osmosis plants by using advanced optimization techniques, Desalin. Water Treat. 10 (2009) 200–209.
[18] L. Sangyoup, C. Jaeweon, M. Elimelech, Influence of colloidal fouling and feed water recovery on salt rejection of RO and NF membranes, Desalination 160 (2004) 1–12.